

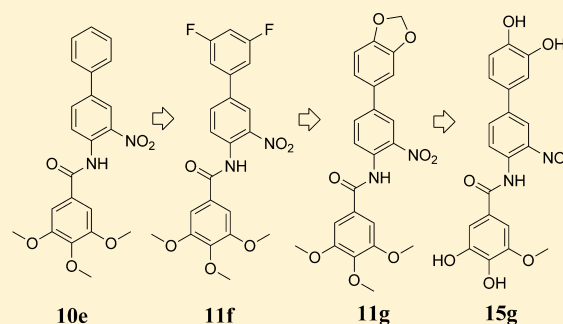
Potent Galloyl-Based Selective Modulators Targeting Multidrug Resistance Associated Protein 1 and P-glycoprotein

Raffaella Zoe Pellicani, Angela Stefanachi, Mauro Niso, Angelo Carotti, Francesco Leonetti, Orazio Nicolotti, Roberto Perrone, Francesco Berardi, Saverio Cellamare,* and Nicola Antonio Colabufo*

Dipartimento Farmaco-Chimico, Università degli Studi di Bari "Aldo Moro", Via Orabona 4, 70125, Bari, Italy

Supporting Information

ABSTRACT: The multifactorial nature of chemotherapy failure in controlling cancer is often associated with the occurrence of multidrug resistance (MDR), a phenomenon likely related to the increased expression of members of the ATP binding cassette (ABC) transporter superfamily. In this respect, the most extensively characterized MDR transporters include ABCB1 (also known as MDR1 or P-glycoprotein) and ABCC1 (also known as MRP1) whose inhibition remains a priority to circumvent drug resistance. Herein, we report how the simple galloyl benzamide scaffold can be easily and properly decorated for the preparation of either MRP1 or P-gp highly selective inhibitors. In particular, some gallamides and pyrogallol-1-monomethyl ethers showed remarkable affinity and selectivity toward MRP1. On the other hand, trimethyl ether galloyl anilides, with few exceptions, exhibited moderate to very high and selective P-gp inhibition.



	10e	11f	11g	15g
IC ₅₀ , MRP1	80 μM	2.5 μM	>100 μM	9.5 μM
IC ₅₀ , P-gp	>100 μM	2.6 μM	0.2 μM	>100 μM

INTRODUCTION

A well-established cause of multidrug resistance (MDR) involves the increased expression of members of the ATP binding cassette (ABC) transporter superfamily, many of which efflux various chemotherapeutic drugs from cells. The most extensively characterized MDR transporters include ABCB1 (also known as MDR1 or P-glycoprotein), ABCC1 (also known as MRP1), and BCRP (also known as ABCG2 or MXR).¹ Multidrug resistance associated proteins (MRPs), in particular, play a key role in cellular protection by effluxing xenobiotics, metabolites, and endogenous substrates that can accumulate in tissues and lead to toxicity. In this respect, MRPs could be considered a double-edged sword: on one hand they play an important role in maintaining cellular homeostasis, while on the other hand, they greatly reduce the intracellular levels of many anticancer drugs.^{2–5}

So far, only limited high-resolution structural information on intact mammalian ABC proteins has been published, mainly related to P-glycoprotein (P-gp) transporter, while no structure-based information on the entire MRP1 has been deposited.⁶ By use of electron microscopy, the structure of MRP1 showed monomers possessing a putative central pore that assembles to form dimers.⁷ Unfortunately, these low-resolution structures have contributed little to the understanding of the complex MRP1's biological machinery. As a result, 3D models for P-gp, MRP1, and BCRP have been created via homology modeling based on a few bacterial ABC proteins.^{8,9}

Many compounds, termed modulators, reversers, inhibitors, or chemosensitizers able to reverse MDR in intact cells *in vitro* by interfering with the ability of the transporter to efflux drugs, have been identified.¹⁰ Although the discovery of the first MDR modulators was serendipitous, in recent years, molecular design, combinatorial chemistry, and the availability of more protein structural information have all played increasingly important roles in identifying more effective compounds.¹¹ While considerable effort has been devoted to developing new P-gp modulators and to deriving convincing pharmacophore patterns, MRP1 inhibitors have not yet been studied to the same extent.^{12,13}

Since the discovery of MRP1 in 1992 by Cole,¹⁴ it had been clear that, except for cyclosporine and verapamil, most P-gp inhibitors (e.g., 1, elacridar; 2, tariquidar; 3, XR9577; Figure 1) did not affect MRP1.^{15,16} Hence, many MRP1 modulators have been studied extensively in recent years, spreading from nonspecific inhibitors of organic anion transporters (e.g., indomethacin and probenecid)^{17,18} and leukotriene receptor antagonists (e.g., 4 (MK571) and 5 (ONO-1078), also termed verlukast and pranlukast, respectively; Figure 1),^{19,20} to tricyclic isoxazoles, which are among the most potent and specific MRP1 inhibitors known to date (e.g., 6 (LY402913) and 7 (LY465803); Figure 1).^{21,22} Additionally, some polyphenolic compounds, including naturally occurring flavonoids such as

Received: September 30, 2011

Published: November 23, 2011

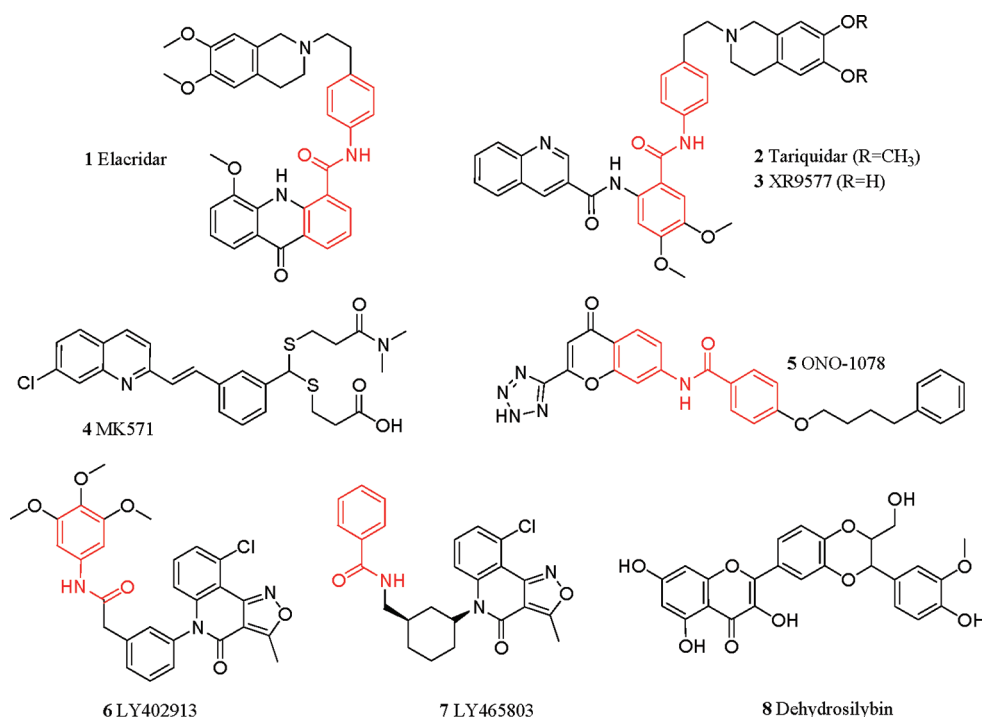
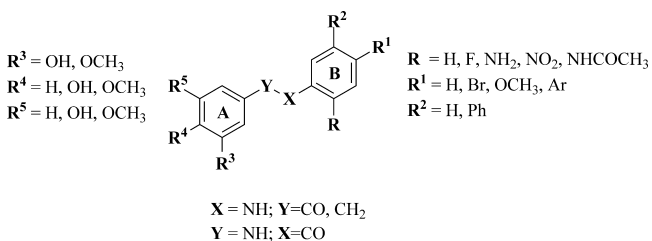


Figure 1. Selected MRP1 inhibitors.

dehydrosilybin (**8**; Figure 1), have been investigated for their ability to modulate MRP1.^{23,24} Despite their molecular similarity, there is still no satisfactory interpretation of the structural requirements of flavonoids necessary for inhibition of MRPs, although some studies, regarding MRP1/2 mediated calcein efflux inhibition, have demonstrated the relevance of having a given ratio between methoxy and hydroxy aromatic substituents.²⁵ Recently, SAR analyses of a tariquidar-based library provided insights on the relevance of selected molecular fragments (i.e., a bulky amine) for the inhibition of breast cancer resistance protein (BCRP), P-gp, and MRP1.^{26,27} There is evidence that a variable alkylphenyl linker incorporating an amide function would be particularly important in MRP1 inhibition. Interestingly, some of these structural motifs are also shared by many P-gp and MRP1 inhibitors, as highlighted in red in Figure 1.

On this rationale, we approached the problem of the intrinsic MRP1 modulatory activity and P-gp selectivity of this common molecular scaffold by designing and testing a small library of polymethoxy-/hydroxy-*N*-phenylbenzamides (Chart 1). As

Chart 1. General Structure of the Designed Compounds (See Table 1)



shown in Chart 1, these compounds retain the trimethoxy or polyphenolic functions seen in many transporter protein

inhibitors, such as 3,4,5-trihydroxybenzoyl (i.e., galloyl) and 3,4- and 3,5-dihydroxybenzoyl moieties.²⁸

First, *N*-biphenyl-4-yl-3,4,5-trimethoxybenzamide derivatives bearing on the B ring (Chart 1) *R* substituents with different stereoelectronic properties were prepared and tested. With the exception of the poor but still appreciable MRP1 inhibition provided by **10e** ($R = \text{NO}_2$), such compounds (i.e., **10a**, **10c**, **10f**) resulted in selective inhibition of P-gp (Table 1). These data led us to explore further R^1 substituents at the 4-position both maintaining the 2-nitro group and preserving the 3,4,5-trimethoxyphenyl moiety (**11a–i**), thereby providing many very active and selective P-gp inhibitors that, only in three cases, were also active against MRP1. Finally, the partial or complete removal of methyl groups from the 3,4,5-trimethoxy fragment, affording pyrogallol-1-monomethyl ethers (**15a–n**) and 3,4,5-trihydroxy (**14a–c**) congeners, respectively, permitted us to gain moderate to good inhibitory activity toward MRP1. Similar reactions were performed in the case of 3,4- and 3,5-dimethoxy congeners (**11l,m**) which gave the catechol (**14d**), 3,5-dihydroxy (**14e**), and isovanillic (**15o**) derivatives.

CHEMISTRY

The synthetic pathways, leading to compounds with the general structures depicted in Table 1, are shown in Schemes 1–4. Variations of *R*, R^1 , and R^2 were accomplished with the choice of substituents by exploring a wide range of stereoelectronic and lipophilic properties. The starting (hetero)arylanilines **9a–j** (Scheme 1) and 3-nitrobiphenyl-4-carboxylic acid (**9k**, Scheme 4) were obtained by Suzuki coupling between the corresponding aniline/carboxylic acid and appropriate arylboronic acids (general procedure in Supporting Information). The physicochemical and spectroscopic data of the known compounds **9a–g** and of trimethoxybenzamides **10b** and **11b** (Scheme 1) fully agreed with those reported in the literature (Tables S1 and S2, respectively, in Supporting Information).^{29,30} The novel synthesized polymethoxy derivatives were prepared by coupling

Table 1. MRP1 and P-gp Inhibitory Activities of Compounds 10a–19^a

compd	X	Y	R	R ¹	R ²	R ³	R ⁴	R ⁵	MRP1 ^b	P-gp ^b
First Subset ^a										
10a	NH	CO	H	Br	H	OCH ₃	OCH ₃	OCH ₃	>100	20.0 ± 3
10b	NH	CO	H	Ph	H	OCH ₃	OCH ₃	OCH ₃	>100	>100
10c	NH	CO	NH ₂	Ph	H	OCH ₃	OCH ₃	OCH ₃	>100	7.2 ± 1
10d	NH	CO	F	Ph	H	OCH ₃	OCH ₃	OCH ₃	>100	1.4 ± 0.5
10e	NH	CO	NO ₂	Ph	H	OCH ₃	OCH ₃	OCH ₃	80 ± 10	>100
10f	NH	CO	NHCOCH ₃	Ph	H	OCH ₃	OCH ₃	OCH ₃	>100	1.9 ± 0.8
Second Subset ^a										
11a	NH	CO	NO ₂	Br	H	OCH ₃	OCH ₃	OCH ₃	>100	>100
11b	NH	CO	NO ₂	OCH ₃	H	OCH ₃	OCH ₃	OCH ₃	>100	>100
11c	NH	CO	NO ₂	H	Ph	OCH ₃	OCH ₃	OCH ₃	>100	0.57 ± 0.1
11d	NH	CO	NO ₂	2-thienyl	H	OCH ₃	OCH ₃	OCH ₃	>100	17.3 ± 2
11e	NH	CO	NO ₂	3-pyridyl	H	OCH ₃	OCH ₃	OCH ₃	6.1 ± 0.8	6.8 ± 1
11f	NH	CO	NO ₂	3,5-difluorophenyl	H	OCH ₃	OCH ₃	OCH ₃	2.5 ± 0.9	2.6 ± 0.7
11g	NH	CO	NO ₂	benzo[1,3]dioxol-5-yl		OCH ₃	OCH ₃	OCH ₃	>100	0.2 ± 0.1
11h	NH	CO	NO ₂	3-acetylphenyl	H	OCH ₃	OCH ₃	OCH ₃	>100	0.6 ± 0.1
11i	NH	CO	NO ₂	3,4,5-(OCH ₃) ₃ Ph	H	OCH ₃	OCH ₃	OCH ₃	11.2 ± 1.5	24.3 ± 2
11j	NH	CO	H	3-nitrophenyl	H	OCH ₃	OCH ₃	OCH ₃	>100	0.4 ± 0.1
11k	NH	CO	NO ₂	3-methylpyridinium iodide	H	OCH ₃	OCH ₃	OCH ₃	>100	34.0 ± 5
11l	NH	CO	NO ₂	Ph	H	H	OCH ₃	OCH ₃	>100	1.3 ± 0.5
11m	NH	CO	NO ₂	Ph	H	OCH ₃	H	OCH ₃	>100	6.6 ± 0.7
12	NH	CH ₂	NO ₂	Ph	H	OCH ₃	OCH ₃	OCH ₃	>100	1.5 ± 0.5
13	CO	NH	NO ₂	Ph	H	OCH ₃	OCH ₃	OCH ₃	>100	2.0 ± 0.5
Third Subset ^a										
14a	NH	CO	NO ₂	Br	H	OH	OH	OH	>100	>100
14b	NH	CO	NO ₂	Ph	H	OH	OH	OH	45.8 ± 10	>100
14c	NH	CO	NO ₂	3-acetylphenyl	H	OH	OH	OH	40.6 ± 18	39.1 ± 7
14d	NH	CO	NO ₂	Ph	H	H	OH	OH	38.8 ± 9	40.3 ± 8
14e	NH	CO	NO ₂	Ph	H	OH	H	OH	46.6 ± 6	72.0 ± 9
Fourth Subset ^a										
15a	NH	CO	NO ₂	Br	H	OH	OH	OCH ₃	44.5 ± 5	38.4 ± 4
15b	NH	CO	NO ₂	OCH ₃	H	OH	OH	OCH ₃	16.3 ± 2	65.0 ± 5
15c	NH	CO	NO ₂	H	Ph	OH	OH	OCH ₃	44.0 ± 3.0	40.2 ± 4
15d	NH	CO	NO ₂	2-thienyl	H	OH	OH	OCH ₃	32.2 ± 1.5	31.2 ± 6
15e	NH	CO	NO ₂	Ph	H	OH	OH	OCH ₃	8.0 ± 1.4	67.0 ± 9
15f	NH	CO	NO ₂	3,5-difluorophenyl	H	OH	OH	OCH ₃	22.0 ± 0.3	16.8 ± 1
15g	NH	CO	NO ₂	3,4-(OH) ₂ Ph	H	OH	OH	OCH ₃	9.5 ± 1	>100
15h	NH	CO	NO ₂	3-acetylphenyl	H	OH	OH	OCH ₃	7.7 ± 1.3	9.1 ± 2
15i	NH	CO	NO ₂	3,4-(OH) ₂ -5-OCH ₃ -Ph	H	OH	OH	OCH ₃	74.5 ± 10	3.1 ± 0.6
15j	NH	CO	H	3-nitrophenyl	H	OH	OH	OCH ₃	40.6 ± 5	32.5 ± 2
15k	NH	CO	H	Ph	H	OH	OH	OCH ₃	75.8 ± 8	>100
15l	NH	CO	NH ₂	Ph	H	OH	OH	OCH ₃	37.9 ± 3.5	>100
15m	NH	CO	F	Ph	H	OH	OH	OCH ₃	30.0 ± 1.5	14.1 ± 1
15n	NH	CO	NHCOCH ₃	Ph	H	OH	OH	OCH ₃	28.0 ± 5.1	>100
15o	NH	CO	NO ₂	Ph	H	H	OCH ₃	OH	>100	3.5 ± 1.5
16	NH	CH ₂	NO ₂	Ph	H	OH	OH	OCH ₃	23.6 ± 3.1	72.0 ± 9
17	CO	NH	NO ₂	Ph	H	OH	OH	OCH ₃	>100	>100
Fifth Subset ^a										
18	NH	CO	NO ₂	Ph	H	<i>o</i> -quinone		OCH ₃	23.3 ± 4	>100
Ver									6.8 ± 3	0.5 ± 0.1
19									17.2 ± 3	31.7 ± 5
MC18 ^c									6.7 ± 0.8	0.8 ± 0.1

Table 1. continued

compd	X	Y	R	R ¹	R ²	R ³	R ⁴	R ⁵	MRP1 ^b	P-gp ^b
MKS71 ^d										
Fifth Subset ^a										
										2.8 ± 0.5

^aCompounds have been assigned to five different structural subsets (see *infra*) and accordingly listed. The first and second subsets present variation at R and R¹. The third subset contains polyhydroxy derivatives. The fourth subset collects pyrogallol 1-methyl ethers, and the fifth one comprises reference compounds, including verapamil (Ver). ^bIC₅₀ data, reported as μM ± SEM, are the mean of two independent experiments, sampled in triplicate. ^cSee ref 37. ^dSee ref 27.

suitable 4-substituted- or 2,4-disubstituted anilines with 3,4- and 3,5-dimethoxy- and 3,4,5-trimethoxybenzoyl chlorides, affording the corresponding benzamides **10a,b** and **10d,e** (Schemes 1 and 2) and **11a–j** and **11l–m** (Schemes 1–3) in good to excellent yields (Table S2 in Supporting Information). The 3-pyridyl congener **11e** was quaternized to form the corresponding methyl iodide salt **11k** (Scheme 3). The *N*-(3,4,5-trimethoxybenzyl)-*N*-(3-nitro-1,1'-biphenyl-4-yl)amine **12** was obtained by a Mitsunobu protocol from 3-nitro-biphenyl-4-ylamine **9e** and 3,4,5-trimethoxybenzyl alcohol (Scheme 1). The reduction of the nitro group in **10e** provided the amino congener **10c** that, in turn, was acetylated to give **10f** (Scheme 2). The *N*-(3,4,5-trimethoxyphenyl)-3-nitro-1,1'-biphenyl-4-carboxamide **13**, which is the reverse-amide-bond isomer of **10e**, was prepared from 4-bromo-2-nitrobenzoic acid, phenylated to yield 3-nitro-1,1'-biphenyl-4-carboxylic acid **9k**, which was then coupled, via its acid chloride, with 3,4,5-trimethoxyaniline (Scheme 4). The final demethylation reactions, affording the corresponding phenols only in low yields, were carried out in two different ways: (1) by using 1 equiv of BBr₃ (1 M in CH₂Cl₂) per methoxy group together with an additional equivalent for the amide function³¹ and (2) by using an excess of BBr₃ (up to 3 equiv per methoxy group).³² With the first protocol, the partial ether cleavage gave, and only in modest yield, 3,4-dihydroxy-5-methoxy derivatives **15a–n**, **16**, **17** as confirmed by 2D NOESY spectra (Figures S1–S7 in Supporting Information). The same protocol furnished the 3-hydroxy-4-methoxy derivatives (isovanilamide) **15o** from the corresponding 3,4-dimethoxybenzamide **11l** (Scheme 2), and no trace was found for the presence of the 4-hydroxy-3-methoxybenzamide regioisomer (vanilamide). The use of the second protocol was necessary to obtain the gallamide derivatives **14a–c** from **11a**, **10e**, and **11h** (Schemes 1–3) and the 3,4- and 3,5-dihydroxybenzamides **14d–e** from **11l–m**, respectively (Scheme 2). The preparation of **19**, a new 3,4-dihydroxy racemic analogue (ring A) of verapamil, was carried out by using a similar demethylation reaction as shown in Scheme 4. To our knowledge, this regioselective transformation, as confirmed by MS spectrum, was not covered by previous studies.^{33–35} Finally, oxidation of **15e**, by using orthochloranil, gave the *o*-quinone derivative **18** (Scheme 2).

BIOCHEMICAL STUDIES

P-gp and MRP1 modulating activities of tested compounds were determined by fluorescence measurements, using calcein-AM fluorescent probes, in MDCK-MDR1 and MDCK-MRP1 cell lines.³⁶ These cells overexpress only P-gp or MRP1 transporters, respectively, so that the observed biological effects can be ascribed to the specific inhibition of these pumps. Calcein-AM is a lipophilic substrate of both P-gp and MRP1 able to cross the cell membrane. Inside the cell compartment, it is hydrolyzed by endogenous cytoplasmic esterases, yielding highly fluorescent calcein. This compound is not a P-gp or

MRP1 substrate, and it cannot cross the cell membrane via passive diffusion because it is too hydrophilic. Thus, a rapid increase in the fluorescence of cytoplasmic calcein can be monitored. P-gp and MRP1 transporters, present in the cell membrane, rapidly efflux the calcein-AM before its entrance into the cytosol, resulting in a reduction of the fluorescent signal due to a decrease in the accumulation of calcein. Evaluation of P-gp or MRP1 activity in the presence of pump inhibitors can be performed in a competitive manner. Compounds that block P-gp and MRP1 pumps inhibit calcein-AM efflux, increasing intracellular accumulation of fluorescent calcein. Values of IC₅₀ for calcein-AM uptake (Table 1) were determined by measuring relative fluorescence values obtained after 30 min of incubation at 37 °C. Typical sigmoidal dose–response curves, regarding MRP1 activity, are shown in Figure 2 in the presence of various concentrations of selected MRP1 and P-gp inhibitors such as **11f** (a trimethoxybenzamide), **14b** (a gallamide), and **15e** (a pyrogallol 1-monomethyl ether). Verapamil and MC18³⁷ were used as reference compounds for MRP1 and P-gp inhibition, respectively. The accuracy and reproducibility of the estimated IC₅₀ values are in accordance with the most recent guidelines.³⁸

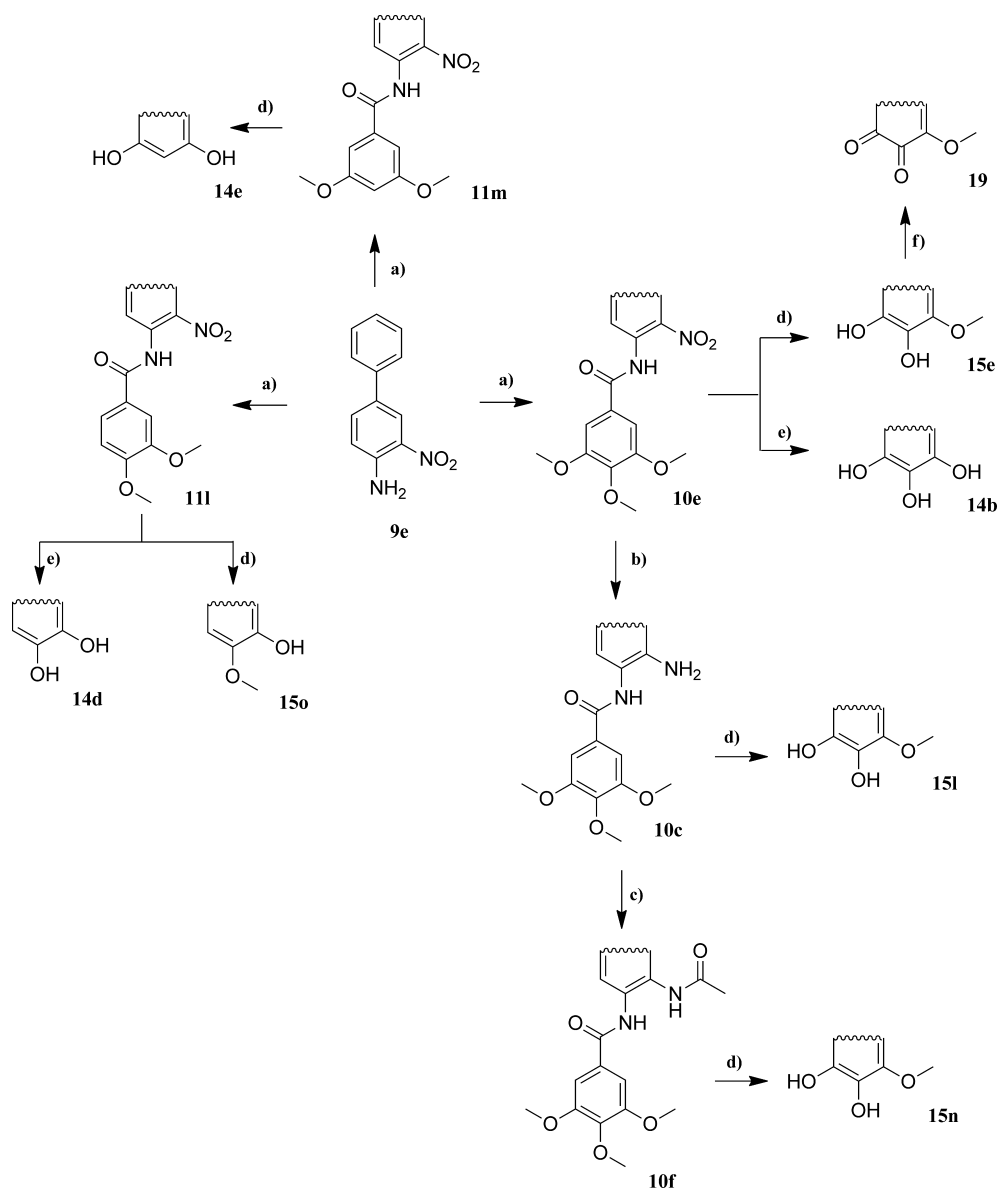
COMPOUND STABILITY ASSAY

Several lines of evidence indicate that catechol type polyphenols can be easily oxidized in a cell culture medium.³⁹ Therefore, we applied an analytical method to test the stability of these compounds, particularly the gallamides and pyrogallol 1-monomethyl ethers, by electron spray ionization/mass spectrometry (ESI-MS). Because of its greater stability in the cell medium at 37 °C, the corresponding trimethoxy congener of each polyphenol derivative (e.g., **10e** vs **14b** or **15e**) was selected as internal standard (IS). First, a linear relationship between inhibitor/internal standard concentration and the molecular ion intensity ratios was established in the 1.0–100 μM range (Figures S8 and S9a–e, Supporting Information). Next, a solution of test compounds and the corresponding IS were added to a stirring culture medium (0.5 mL) at 37 °C to yield the final concentration in the desired range, and sampling at 15, 30, 60, and 90 min after start was made. The relative concentrations of polyphenols were ultimately measured by comparing the ratio of the respective molecular ion intensities and that of the IS (Figure S10a–d, Supporting Information). All tested phenols proved to be stable for at least 1 h in the assay conditions (Figure S11, Supporting Information).

RESULTS AND DISCUSSION

In the search for novel and selective transporter protein inhibitors, a small series of 3,4,5-trimethoxy-*N*-phenylbenzamide derivatives (i.e., **10a–f**, first subset of Table 1), whose general structure is depicted in Chart 1, was designed and

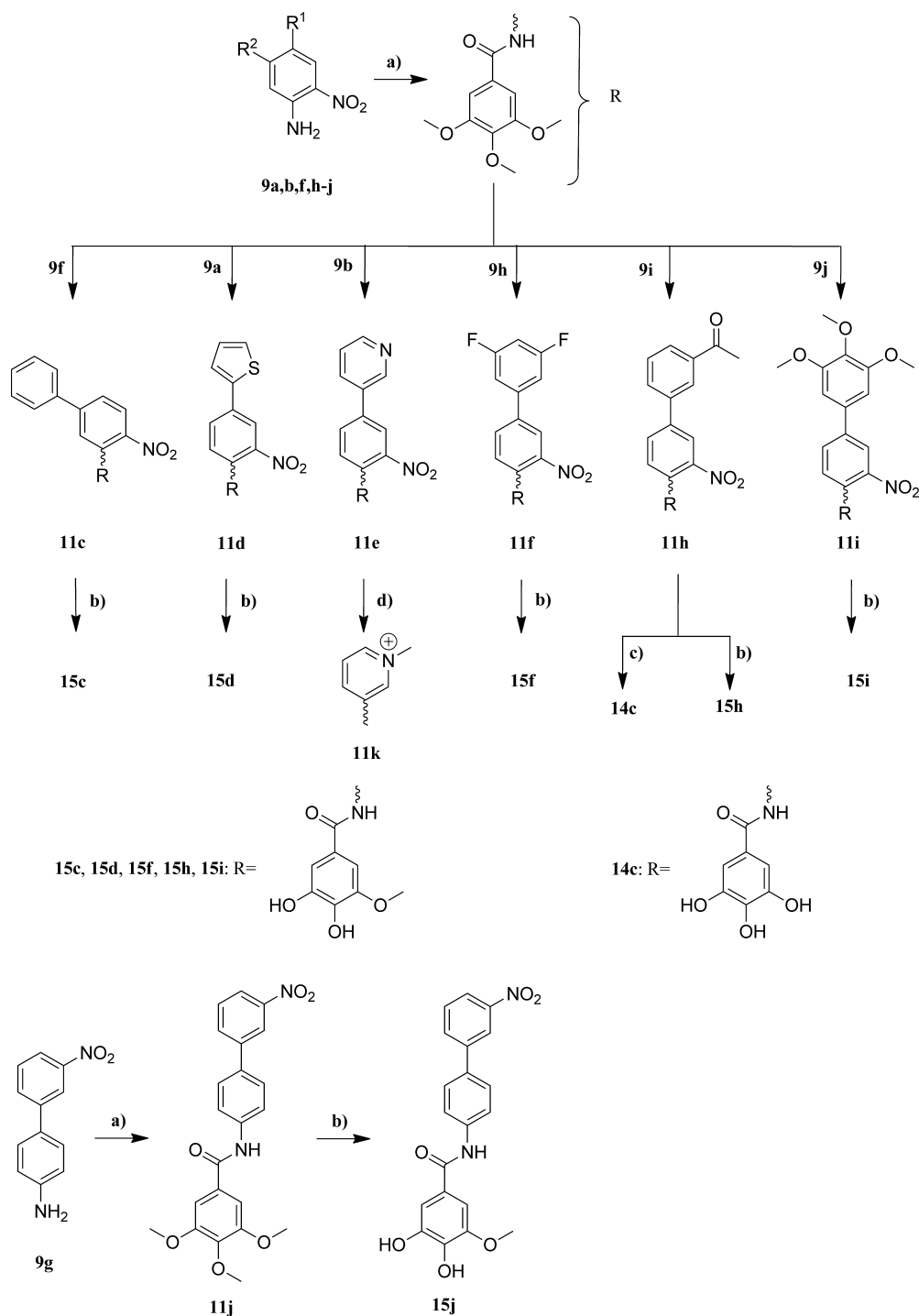
Scheme 2. Synthesis of Trimethoxybenzamides 10,c,e,f, 11l,m, 3,4- and 3,5-Dihydroxybenzoyl Derivatives 14d–e, Isovanilloyl Derivative 15o, Galloyl Derivative 14b, Pyrogallol 1-Monomethyl Ether Congeners 15e,l,n, and *o*-Quinone 19^a



^aReagents and conditions: (a) appropriate benzoyl chloride, dry 1,4-dioxane and DMF, microwave irradiation (25 min, 130 °C, $E_{\max} = 500$ W); (b) Pd/C (10% w/w) under H₂ atmosphere, absolute ethanol, room temp, 12 h; (c) acetic anhydride, DMAP, 1,4-dioxane, room temp, 24 h; (d) BBr₃ (1 M in DCM), 4 equiv, dry DCM, -40 °C → room temp, 2 h; (e) BBr₃ (1 M in DCM), 6–9 equiv, dry DCM, -40 °C → room temp, 6 h; (f) orthochloranil, THF, -30 °C, 2 h.

tested. Despite the consistent spread of the electronic (Hammett σ) and lipophilic (π) parameters of the explored R and, to a lesser extent, R¹ substituents, the only compound indicating an appreciable inhibitory activity against MRP1, and devoid of any detectable P-gp inhibition (Table 1), was the nitro derivative 10e ($IC_{50} = 80 \mu\text{M}$). The other benzamides of this subset (10a–d and 10f) showed, conversely, moderate to good P-gp inhibition with IC_{50} values from 20 to 1.4 μM . These intriguing and somehow unexpected outcomes led us to pursue the study with two parallel approaches: (i) keeping fixed the 3,4,5-trimethoxy-*N*-(2-nitrophenyl)benzamide scaffold and introducing a series of R¹ substituents in the 4'-position of the aniline moiety to afford a second subset of compounds (11a–m) and (ii) demethylating one or more methoxy groups on the ring A to afford a third and a fourth subset comprising

gallamide (14a–c) and pyrogallol 1-monomethyl ether derivatives (15a–n), respectively (Table 1). The biological screening of the second subset returned the promising, although nonactive, MRP1 inhibitors 11e, 11f, and 11i, showing IC_{50} values equal to 6.1, 2.5, and 11.2 μM , respectively. These good activities might be ascribed to the presence in the 4'-position of aryl groups that may act as strong HB acceptors. Unfortunately, this interpretation did not hold for the benzo[1,3]dioxol-5-yl derivative 11g that exhibited no MRP1 inhibition. The quaternization of the 4'-(3-pyridyl) derivative 11e led to the totally inactive methyl iodide 11k (MRP1 $IC_{50} > 100 \mu\text{M}$). Even though we cannot exclude the possibility that the significant drop of lipophilicity may limit cell membrane penetration of 11k, its P-gp inhibitory activity seemed to be preserved, though moderate ($IC_{50} = 34 \mu\text{M}$).

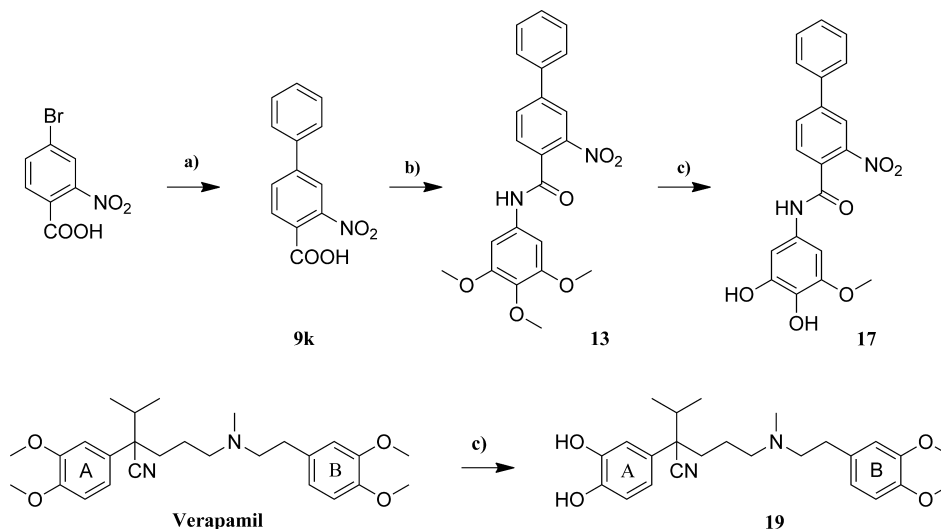
Scheme 3. Synthesis of Trimethoxybenzamides 11c–f,h–j, Galloyl Derivative 14c, Pyrogallol 1-Monomethyl Ether Congeners 15c,d,f,h–j, and the Methylpyridinium Iodide Derivative 11k^a

^aReagents and conditions: (a) 3,4,5-trimethoxybenzoyl chloride, dry 1,4-dioxane and DMF, microwave irradiation (25 min, 130 °C, $E_{\max} = 500$ W); (b) BBr_3 (1 M in DCM), 4 equiv, dry DCM, -40 °C \rightarrow room temp, 2 h; (c) BBr_3 (1 M in DCM), 6–9 equiv, dry DCM, -40 °C \rightarrow room temp, 6 h; (d) CH_3I , 6 equiv, acetonitrile–dry DCM (2/1, v/v), 50 °C, 2 h.

With the exception of the 4'-bromo- and 4'-methoxy congeners (11a,b) all compounds of this subset were moderate to very potent and selective P-gp inhibitors. In particular, the IC_{50} values of 11c, 11g, 11h, and 11j were in the submicromolar range. Taken together, these data seem to corroborate the distinctive role of the trimethoxyphenyl moiety recurring in many MDR modulators.⁴⁰

The screening of the gallamide derivatives 14a–e (third subset in Table 1) indicated a moderate inhibitory potency for both MRP1 and P-gp, irrespective of the number and position of the phenolic groups. Compound 14a, lacking the 4'-phenyl group, was completely inactive, while 14b showed a weak MRP1 selectivity.

Finally, the last series of structural modifications implying the partial cleavage of the methoxy groups afforded the more

Scheme 4. Synthesis of Trimethoxycarboxamide 13, 3,4-Dihydroxy-5-methoxyphenyl Derivative 17, and Cathecol Derivative 19^a

^aReagents and conditions: (a) phenylboronic acid, Pd(Ph₃)₄, aq K₂CO₃ (2 M), DMF, reflux, 3 h; (b) (1) SOCl₂, reflux, 2 h; (2) 3,4,5-trimethoxyaniline, dry 1,4-dioxane/DMF, microwave irradiation (25 min, 130 °C, E_{\max} = 500 W); (c) BBr₃ (1 M in DCM), 4 equiv, dry DCM, -40 °C → room temp, 3 h.

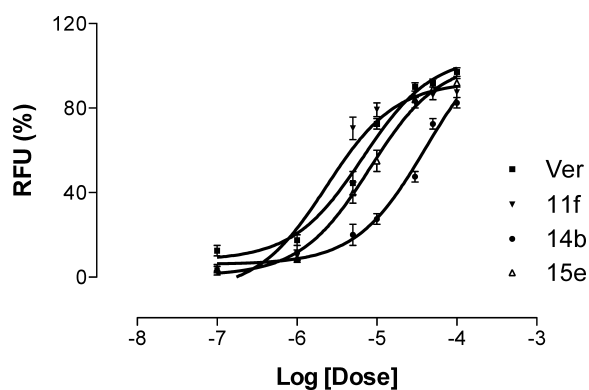


Figure 2. Representative curves for the MRP1 inhibitory activities of selected compounds and verapamil (Ver), carried out with calcein-AM assay in MDCK-MRP1 cell lines: (▼) 11f, IC_{50} = 2.5 ± 0.9 μM; (●) 14b, IC_{50} = 45.8 ± 10 μM; (△) 15e, IC_{50} = 8.0 ± 1.4 μM; (■) Ver, IC_{50} = 6.8 ± 3 μM. Each compound has been tested at seven concentrations (from 0.1 to 100 μM), each concentration in triplicate in two independent experiments. The y-axis indicates the percentage of RFU (relative fluorescence unit). Statistical analysis has been performed with the Friedman test (P = 0.0078, significant; Friedman statistic value of 11.87).

hydrophilic pyrogallol 1-monomethyl ether derivatives 15a–n (fourth subset in Table 1), all showing moderate to good inhibition activity toward both transporters.

The *o*-NO₂ derivative 15e exhibited higher MRP1 inhibitory activity (IC_{50} = 8.0 μM) compared to the unsubstituted compound 15k (IC_{50} = 75.8 μM) and the corresponding *o*-NH₂ 15l (IC_{50} = 37.9 μM) and *o*-NHCOCH₃ 15n (IC_{50} = 28.5 μM) derivatives. With the interesting exception of compound 15g (IC_{50} = 9.5 and >100 μM toward MRP1 and P-gp respectively), the selectivity of these compounds was quite moderate.

The replacement of the phenyl ring in 15e with the 2-thienyl isoster gave 15d, whose MRP1 affinity was decreased (IC_{50} increased from 8.0 to 32 μM) while the corresponding trimethoxybenzamide (11d) was inactive toward the same

protein transporter. The replacement of the 4'-phenyl ring of 15e with substituents showing different stereoelectronic and lipophilic properties (i.e., R¹ = Br and OCH₃, in 15a,b, respectively) led to a reduction of activity, more pronounced in the bromo derivative 15a (IC_{50} = 44.5 μM).

Taking into account that the most important inhibitory activity changes were mainly concerned with the structural modifications on ring B, the role of the amide bond linking the A and B aromatic rings was investigated. To this end, two analogues of compound 15e were prepared: the first with a reverse amide bond (i.e., from NHCO to CONH); the second with a reduced amide bond (i.e., from NHCO to NHCH₂). Compound 16, bearing the reduced amide bond as a linker, retained, at least in part, the activity of parent compound 15e toward MRP1 and was equipotent toward P-gp despite the drastic change in terms of planarity and conformational flexibility. Moreover, compound 17 having the reverse amide bond showed no inhibitory activity toward both MRP1 and P-gp. The 3,4,5-trimethoxybenzamide analogues 12 and 13, bearing the NHCH₂ and CONH linkers, respectively, were inactive toward MRP1 while displaying a high and close inhibitory potency toward P-gp (IC_{50} equal to 1.5 and 2.0 μM, respectively).

Since at the cellular level the catechol moiety of 15e might be oxidized to the corresponding *o*-quinone derivative 18, this possible metabolite was prepared and tested. It showed a significantly lower inhibitory activity toward both protein transporters.

Finally, the change of activity arising from the presence of a catechol moiety was further challenged with the selective bis-demethylation of the verapamil, a well-known golden standard of P-gp dependent MDR reverters.⁴³ Disappointingly, the new catechol derivative 19 (Scheme 4) showed lower inhibitory activity than the parent compound toward both MRP1 and P-gp.

In Figure 2, representative activity curves, regarding MRP1 activity, of compounds 11f, 14b, and 15e, the best MRP1 ligands with similar P-gp potency (11f), P-gp inactivity (14f), or moderate selectivity (15e), were inserted.

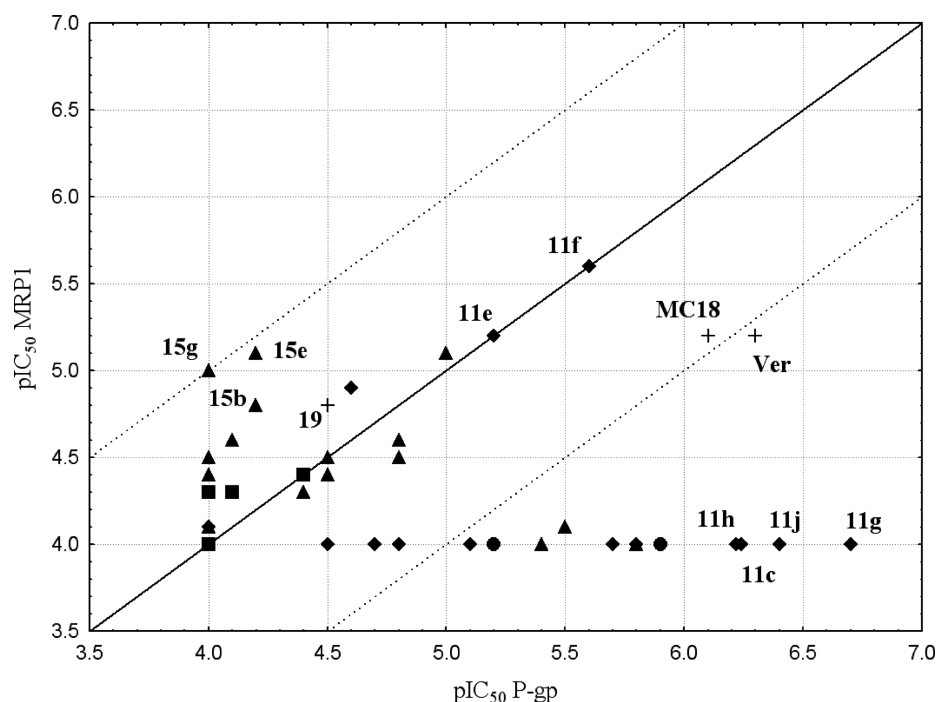


Figure 3. Square plot of P-gp/MRP1 inhibition data (Table 1): (◆) trimethoxybenzamides (10a, 11f, 11a–k, 12, 13); (■) gallamides and other polyphenols (14a–e); (▲) pyrogallol 1-monomethyl ethers (15a–o, 16) and 17; (●) dimethoxybenzamides (11l, 11m); (+) reference compounds and 19. The solid line represents the bisector, while the dotted lines, traced at the 1 log unit distance above and below the bisector, help to identify selective compounds.

For ease of interpretation, the inhibition data are presented in Figure 3 as a square plot of P-gp (*x*-axis) versus MRP1 (*y*-axis) pIC_{50} values. To avoid the lack of valuable information, inhibition data of inactive compounds ($IC_{50} > 100 \mu M$) were reported with an arbitrary cut value ($pIC_{50} = 4.0$). Compounds with equal affinities for both transporters lie on the bisector ($y = x$) of the graph, whereas selective P-gp and MRP1 inhibitors lie below and above the bisector, respectively. The distance of their pIC_{50} values from the bisector is a direct measure of their degree of selectivity. The plotted data indicate that the trimethoxybenzamides 11c,g–j are potent and selective P-gp inhibitors, with $pIC_{50} < 6$. These compounds showed no MRP1 activity that can be successfully recovered but at the expense of selectivity by introducing strong HB acceptor groups (11e,f). To gain selectivity for MRP1, phenolic groups need to be restored as in the pyrogallol 1-monomethyl ethers (15e, 15g). However, the potency and selectivity of these compounds did not rise up to the best P-gp inhibitors.

Despite a relatively large variation of several physicochemical features (such as molecular lipophilicity spanning a 2.3 log unit range) and structural features (i.e., phenyl substitution patterns, regioisomerism, and isosterism), no clear SAR emerged from a thorough analysis of all inhibition data. Nevertheless, a trend between lipophilicity and P-gp modulation of the most active compounds was observed as shown in Figure 4. The modulation of MRP1, on the contrary, appears to be insensitive to the lipophilicity.

CONCLUSIONS

Our results demonstrate the versatile nature of the galloyl benzamide scaffold for preparing very active MRP1 and P-gp inhibitors. Simple chemical modifications were able to switch over the selectivity while keeping high potency. In particular, the potent and very selective P-gp inhibitor 11g, a galloyl

trimethyl ether derivative, can be easily converted in its polyphenolic congener 15g, a quite selective MRP1 modulator. Furthermore, a thorough modulation of the inhibition potency was obtained by means of suitable substitutions on the B ring, thus biasing P-gp and MRP1 with IC_{50} values encompassing 2 and 1 order of magnitude, respectively. Finally, from a careful tuning of the chemical decoration through demethylation reaction and introduction of selected HB acceptor groups on the phenyl fragment bonded to the B ring, dual active MDR modulators were discovered (e.g., 11e,f).

These encouraging results allow us to consider the galloyl benzamide as a versatile scaffold for designing promising P-gp and MRP1 modulators. Further biochemical and pharmacological studies to better define the interaction mechanism responsible for the observed selectivity and an exploration of the therapeutic potential of these compounds as MDR reversers are warranted.

EXPERIMENTAL SECTION

Chemistry. High analytical grade chemicals and solvents were from commercial suppliers. When necessary, solvents were dried by standard techniques and distilled. After extraction from aqueous layers, the organic solvents were dried over anhydrous sodium sulfate. Thin layer chromatography (TLC) was performed on aluminum sheets precoated with silica gel 60 F254 (0.2 mm) (E. Merck).

Chromatographic spots were visualized by UV light. Purification of crude compounds was carried out by flash column chromatography on silica gel 60 (Kieselgel 0.040–0.063 mm, E. Merck) or by preparative TLC on silica gel 60 F254 plates or crystallization. 1H NMR spectra were recorded in $DMSO-d_6$ at 300 MHz on a Varian Mercury 300 instrument. Chemical shifts (δ scale) are reported in parts per million (ppm) relative to the central peak of the solvent. Coupling constant (J values) are given in hertz (Hz). Spin multiplicities are given as s (singlet), br s (broad singlet), d (doublet), t (triplet), dd (double doublet), dt (double triplet), or m (multiplet). LRMS (ESI) was

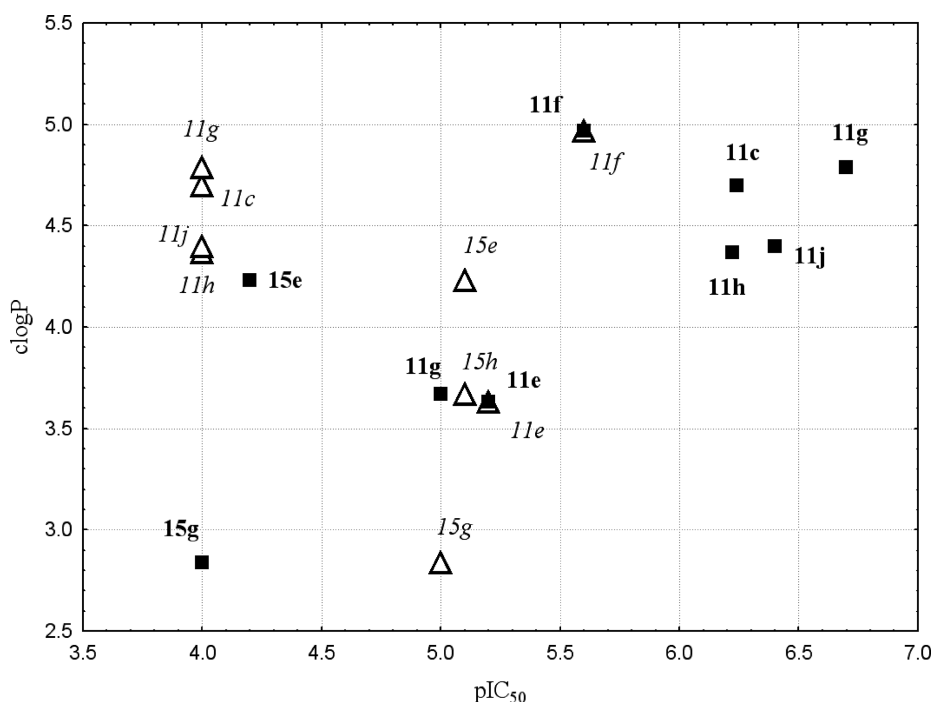


Figure 4. Relationships of the most relevant inhibition data (Table 1) versus clogP data. The pIC₅₀ data relative to MRP1 and P-gp are represented as empty upside triangles (italic labels) and solid squares (bold labels), respectively. The clogP values have been calculated by using ACD software.

performed with an electrospray interface ion trap mass spectrometer (1100 series LC/MSD trap system Agilent, Palo Alto, CA). In all cases, spectroscopic data are in agreement with known compounds and assigned structures. Combustion analyses were performed by Eurovector Euro EA 3000 analyzer (Milan, Italy) and gave satisfactory results (C, H, N within 0.4% of calculated values). HPLC purity determinations were carried out using a Phenomenex PhenoSphere-Next C8 150 mm × 4.6 mm column, with 5 μm particle size: isocratic 1 (for polyphenolic derivatives **14a–e**, **15a–o**, **16**, **17**), 10 mM ammonium acetate in H₂O/MeOH, 70/30, v/v, room temp; isocratic 2 (for trimethyl ether galloyl anilides and dimethoxy derivatives **10a–f**, **11a–m**, **12**, **13**), 10 mM ammonium acetate in H₂O/MeOH, 55/45, v/v, room temp. All test compounds were confirmed to be ≥95% pure by HPLC.

General procedures for the Suzuki–Miyaura cross-coupling reaction (**9a–k**, **11g**) and benzoylation reaction (**10a,b,d,e**, **11a–j,l,m**, and **13**) are reported in Supporting Information.

Procedures for the catalytic hydrogenation (**10c**), acetylation reaction (**10f**), quaternization reaction (**11k**), and Mitsunobu reaction (**12**) are reported in Supporting Information.

General Procedure for the Preparation of Phenol Derivatives 14a–e, 15a–o, 16, 17, and 19. Suitable benzamide (0.50 mmol) was dissolved in dry DCM (30 mL) under argon and cooled at –40 °C. Boron tribromide (BBr₃, 1 M in DCM), 2.0 mL (2.0 mmol for compounds **15a–o**, **16**, **17**, **19**) and 3.0–4.5 mL (3.0–4.5 mmol for compounds **14a–e**), was added dropwise, and the mixture was stirred for 2 h. After the reaction was quenched with 50 mL of H₂O, the desired phenol was obtained through two different procedures. When the phenol precipitated from the reaction mixture, it was recovered by filtration (**15a,e,g,h,i,k,n**). In all other cases, the aqueous phase was extracted with DCM and the organic phase was first dried over anhydrous Na₂SO₄ and then evaporated under vacuum to dryness affording the desired product. Except for **15a,b,e,m**, all the phenolic compounds were purified by preparative thin layer chromatography (TLC) as specified below.

N-(4-Bromo-2-nitrophenyl)-3,4,5-trihydroxybenzamide (14a). Purification by preparative TLC yielded **14a** (38 mg, 21%): mp 185 °C dec. ¹H NMR (DMSO-*d*₆): δ = 10.49 (s, 1H), 9.08 (br s, 3H), 8.16 (d, *J* = 2.2 Hz, 1H), 7.91 (dd, *J* = 2.2 Hz, *J* = 8.8 Hz, 1H), 7.83 (d, *J* = 8.8 Hz, 1H), 6.91 (s, 2H). LRMS (ESI) *m/z* 368 [M – H][–].

3,4,5-Trihydroxy-N-(3-nitrophenyl-4-yl)benzamide (14b). Purification by preparative TLC yielded **14b** (18 mg, 6%): mp 175 °C dec. ¹H NMR (DMSO-*d*₆): δ: 10.52 (s, 1H), 9.05 (br s, 3H), 8.23 (s, 1H), 8.03 (s, 2H), 7.75 (d, *J* = 7.2 Hz, 2H), 7.50 (t, *J* = 7.2 Hz, 2H), 7.42 (d, *J* = 7.2 Hz, 1H), 6.95 (s, 2H). LRMS (ESI) *m/z* 365 [M – H][–].

N-(3'-Acetyl-3-nitrophenyl-4-yl)-3,4,5-trihydroxybenzamide (14c). Purification by preparative TLC yielded **14c** (30 mg, 15%): mp 180 °C dec. ¹H NMR (DMSO-*d*₆): δ: 8.33 (s, 1H), 8.28 (s, 1H), 8.12 (s, 2H), 8.02 (d, *J* = 7.8 Hz, 1H), 7.98 (s, 1H), 7.64 (t, *J* = 7.8 Hz, 1H), 7.07 (s, 1H), 7.02 (s, 1H), 5.4 (br s, 1H), 3.6 (br s, 3H), 3.75 (s, 3H). LRMS (ESI) *m/z* 407 [M – H][–].

3,4-Dihydroxy-N-(3-nitrophenyl-4-yl)benzamide (14d). Purification by preparative TLC yielded **14d** (47 mg, 27%): mp 175–177 °C. ¹H NMR (DMSO-*d*₆): δ: 10.54 (s, 1H), 9.50 (br s, 2H), 8.23 (d, *J* = 1.7 Hz, 1H), 8.05 (dd, *J* = 1.7, 8.5 Hz, 1H), 7.95 (d, *J* = 8.5 Hz, 1H), 7.76 (d, *J* = 7.2 Hz, 2H), 7.50 (t, *J* = 7.2 Hz, 2H), 7.42 (d, *J* = 7.2 Hz, 1H), 7.37 (s, 1H), 7.34 (d, *J* = 8.0 Hz, 1H), 6.86 (d, *J* = 8.0 Hz, 1H). LRMS (ESI) *m/z* 349 [M – H][–].

3,4-Dihydroxy-N-(3-nitrophenyl-4-yl)benzamide (14e). Purification by preparative TLC yielded **14e** (26 mg, 15%): mp 250–252 °C. ¹H NMR (DMSO-*d*₆): δ: 10.63 (s, 1H), 9.66 (s, 2H), 8.23 (d, *J* = 2.2 Hz, 1H), 8.05 (dd, *J* = 2.2, 8.5 Hz, 1H), 7.93 (d, *J* = 8.5 Hz, 1H), 7.76 (d, *J* = 7.2 Hz, 2H), 7.50 (t, *J* = 7.2 Hz, 2H), 7.43 (d, *J* = 7.2 Hz, 1H), 6.79 (d, *J* = 1.9 Hz, 2H), 6.44 (d, *J* = 1.9 Hz, 1H). LRMS (ESI) *m/z* 349 [M – H][–].

N-(4-Bromo-2-nitrophenyl)-3,4-dihydroxy-5-methoxybenzamide (15a). Recrystallization from EtOH yielded **15a** (124 mg, 65%): mp 206–208 °C. ¹H NMR (DMSO-*d*₆): δ: 10.52 (s, 1H), 9.33 (s, 1H), 9.13 (s, 1H), 8.17 (d, *J* = 2.2 Hz, 1H), 7.93 (dd, *J* = 2.2, 8.8 Hz, 1H), 7.74 (d, *J* = 8.8 Hz, 1H), 7.08 (s, 2H), 3.82 (s, 3H). LRMS (ESI) *m/z* 382 [M – H][–].

3,4-Dihydroxy-5-methoxy-N-(4-methoxy-2-nitrophenyl)-benzamide (15b). Recrystallization from EtOH yielded **15b** (100 mg, 61%): mp 176–178 °C. ¹H NMR (DMSO-*d*₆): δ: 10.25 (s, 1H), 9.26 (s, 1H), 9.03 (s, 1H), 7.63 (d, *J* = 9.1 Hz, 1H), 7.49 (d, *J* = 2.5 Hz, 1H), 7.74 (dd, *J* = 2.5, 9.1 Hz, 1H), 7.08 (s, 2H), 3.83 (s, 3H), 3.81 (s, 3H). LRMS (ESI) *m/z* 333 [M – H][–].

3,4-Dihydroxy-5-methoxy-N-(4-nitrophenyl-3-yl)-benzamide (15c). Purification by preparative TLC yielded **15c** (19 mg, 10%): mp 230–233 °C. ¹H NMR (DMSO-*d*₆): δ: 10.62 (s, 1H),

9.36 (s, 1H), 9.16 (s, 1H), 8.21 (s, 1H), 8.10 (d, $J = 8.5$ Hz, 1H), 7.75 (d, $J = 8.0$ Hz, 2H), 7.66 (d, $J = 8.5$ Hz, 1H), 7.53 (t, $J = 8.0$ Hz, 2H), 7.48 (d, $J = 8.0$ Hz, 1H), 7.12 (s, 2H), 3.83 (s, 3H). LRMS (ESI) m/z 379 $[M - H]^-$.

3,4-Dihydroxy-5-methoxy-*N*-(2-nitro-4-thiophen-2-ylphenyl)benzamide (15d). Purification by preparative TLC yielded 15d (18 mg, 8%): mp 165 °C dec. $^1\text{H NMR}$ (DMSO- d_6) δ : 10.54 (s, 1H), 8.27 (d, $J = 2.2$ Hz, 1H), 8.08 (dd, $J = 2.2, 8.5$ Hz, 1H), 7.95 (d, $J = 8.5$ Hz, 1H), 7.75 (d, $J = 3.6$ Hz, 1H), 7.72 (d, $J = 5.0$ Hz, 1H), 7.26 (dd, $J = 3.6, 5.0$ Hz, 1H), 7.18 (s, 2H), 5.05 (br s, 2H), 3.91 (s, 3H). LRMS (ESI) m/z 385 $[M - H]^-$.

3,4-Dihydroxy-5-methoxy-*N*-(3-nitrobiphenyl-4-yl)-benzamide (15e). Purification by preparative TLC yielded 15e (95 mg, 50%): mp 159 °C dec. $^1\text{H NMR}$ (DMSO- d_6) δ : 10.55 (s, 1H), 9.34 (s, 1H), 9.12 (s, 1H), 8.23 (d, $J = 2.2$ Hz, 1H), 8.05 (dd, $J = 2.2, 8.5$ Hz, 1H), 7.91 (d, $J = 8.5$ Hz, 1H), 7.76 (d, $J = 7.2$ Hz, 2H), 7.50 (t, $J = 7.2$ Hz, 2H), 7.42 (d, $J = 7.2$ Hz, 1H), 7.12 (s, 2H), 3.83 (s, 3H). LRMS (ESI) m/z 379 $[M - H]^-$.

***N*-(3',5'-Difluoro-3-nitrobiphenyl-4-yl)-3,4-dihydroxy-5-methoxybenzamide (15f)**. Purification by preparative TLC yielded 15f (31 mg, 15%): mp 182 °C dec. $^1\text{H NMR}$ (DMSO- d_6) δ : 10.60 (s, 1H), 8.38 (s, 1H), 8.12 (d, $J = 8.7$ Hz, 1H), 7.96 (d, $J = 8.4$ Hz, 1H), 7.60 (s, 2H), 7.58 (s, 1H), 7.27 (m, 1H), 7.15 (m, 1H), 5.12 (br s, 2H), 3.84 (s, 3H). LRMS (ESI) m/z 415 $[M - H]^-$.

***N*-(3',4'-Dihydroxy-3-nitrobiphenyl-4-yl)-3,4-dihydroxy-5-methoxybenzamide (15g)**. Purification by preparative TLC yielded 15g (51 mg, 25%): mp 235 °C dec. $^1\text{H NMR}$ (DMSO- d_6) δ : 10.45 (s, 1H), 8.05 (s, 1H), 7.95–7.80 (m, 2H), 7.17–7.02 (m, 4H), 6.83 (d, $J = 8.3$ Hz, 1H), 6.50 (br s, 2H), 5.45 (br s, 2H), 3.82 (s, 3H). LRMS (ESI) m/z 411 $[M - H]^-$.

***N*-(3'-Acetyl-3-nitrobiphenyl-4-yl)-3,4-dihydroxy-5-methoxybenzamide (15h)**. Purification by preparative TLC yielded 15h (25 mg, 12%): mp 202–205 °C. $^1\text{H NMR}$ (DMSO- d_6) δ : 8.33 (s, 1H), 8.28 (s, 1H), 8.12 (s, 2H), 8.02 (d, $J = 9.6$ Hz, 1H), 7.98 (d, $J = 9.6$ Hz, 1H), 7.65 (d, $J = 7.8$ Hz, 1H), 7.63 (d, $J = 7.8$ Hz, 1H), 7.07 (s, 1H), 7.02 (s, 1H), 5.25 (br s, 2H), 3.75 (s, 3H), 2.67 (s, 3H). LRMS (ESI) m/z 421 $[M - H]^-$.

***N*-(3',4'-Dihydroxy-5'-methoxy-3-nitrobiphenyl-4-yl)-3,4-dihydroxy-5-methoxybenzamide (15i)**. Purification by preparative TLC yielded 15i (26 mg, 12%): mp 240 °C dec. $^1\text{H NMR}$ (DMSO- d_6) δ : 10.46 (s, 1H), 9.07 (br s, 4H), 8.10 (d, $J = 1.9$ Hz, 1H), 7.93 (dd, $J = 1.9, 8.5$ Hz, 1H), 7.82 (d, $J = 8.5$ Hz, 1H), 7.10 (s, 2H), 6.83 (d, $J = 1.7$ Hz, 1H), 6.77 (d, $J = 1.7$ Hz, 1H), 3.84 (s, 3H), 3.83 (s, 3H). LRMS (ESI) m/z 441 $[M - H]^-$.

3,4-Dihydroxy-5-methoxy-*N*-(3'-nitrobiphenyl-4-yl)-benzamide (15j). Purification by preparative TLC yielded 15j (38 mg, 20%): mp 180 °C dec. $^1\text{H NMR}$ (DMSO- d_6) δ : 10.08 (s, 1H), 9.11 (s, 2H), 8.43 (s, 1H), 8.18–8.13 (m, 2H), 7.91 (d, $J = 8.8$ Hz, 2H), 7.78 (d, $J = 8.8$ Hz, 2H), 7.73 (t, $J = 8.3$ Hz, 1H), 7.13 (d, $J = 2.5$ Hz, 2H), 3.84 (s, 3H). LRMS (ESI) m/z 379 $[M - H]^-$.

***N*-Biphenyl-4-yl-3,4-dihydroxy-5-methoxybenzamide (15k)**. Purification by preparative TLC yielded 15k (16 mg, 8%): mp 165 °C dec. $^1\text{H NMR}$ (DMSO- d_6) δ : 9.42 (s, 1H), 7.94 (d, $J = 8.8$ Hz, 2H), 7.70–7.61 (m, 4H), 7.45 (t, $J = 7.4$ Hz, 2H), 7.34 (d, $J = 7.4$ Hz, 1H), 7.24 (d, $J = 1.9$ Hz, 2H), 5.70 (br s, 2H), 3.89 (s, 3H). LRMS (ESI) m/z 334 $[M - H]^-$.

***N*-(3-Aminobiphenyl-4-yl)-3,4-dihydroxy-5-methoxybenzamide (15l)**. Purification by preparative TLC yielded 15l (93 mg, 53%): mp 192 °C dec. $^1\text{H NMR}$ (DMSO- d_6) δ : 9.46 (s, 1H), 7.57 (d, $J = 7.3$ Hz, 2H), 7.42 (t, $J = 7.3$ Hz, 2H), 7.32 (d, $J = 7.3$ Hz, 1H), 7.22 (d, $J = 8.1$ Hz, 1H), 7.14 (s, 1H), 7.12 (s, 1H), 7.06 (d, $J = 1.8$ Hz, 1H), 6.05 (br s, 2H), 6.88 (dd, $J = 1.8, 8.1$ Hz, 1H), 4.96 (s, 2H), 3.82 (s, 3H). LRMS (ESI) m/z 349 $[M - H]^-$.

***N*-(3-Fluorobiphenyl-4-yl)-3,4-dihydroxy-5-methoxybenzamide (15m)**. Recrystallization from EtOH yielded 15m (24 mg, 14%): mp 225–228 °C. $^1\text{H NMR}$ (DMSO- d_6) δ : 9.84 (s, 1H), 9.21 (s, 1H), 8.96 (s, 1H), 7.71 (d, $J = 7.2$ Hz, 2H), 7.63 (d, $J = 8.3$ Hz, 1H), 7.58 (d, $J = 1.7$ Hz, 1H), 7.51 (dd, $J = 1.7, 8.3$ Hz, 1H), 7.46 (t, $J = 7.2$ Hz, 2H), 7.38 (d, $J = 7.2$ Hz, 1H), 7.16 (s, 1H), 7.14 (s, 1H), 3.83 (s, 3H). LRMS (ESI) m/z 352 $[M - H]^-$.

***N*-(3-Acetylamino-biphenyl-4-yl)-3,4-dihydroxy-5-methoxybenzamide (15n)**. Recrystallization from EtOH yielded 15n (22 mg, 11%): mp 235 °C dec. $^1\text{H NMR}$ (DMSO- d_6) δ : 9.88 (s, 1H), 9.66 (s, 1H), 9.26 (s, 1H), 9.03 (s, 1H), 7.77 (d, $J = 8.3$ Hz, 1H), 7.71 (s, 1H), 7.64 (d, $J = 7.7$ Hz, 2H), 7.57–7.41 (m, 3H), 7.37 (d, $J = 7.4$ Hz, 1H), 7.09 (s, 2H), 3.83 (s, 3H), 2.21 (s, 3H). LRMS (ESI) m/z 391 $[M - H]^-$.

3-Hydroxy-4-methoxy-*N*-(3-nitrobiphenyl-4-yl)benzamide (15o). Recrystallization from EtOH yielded 15o (47 mg, 26%): mp 195–198 °C. $^1\text{H NMR}$ (DMSO- d_6) δ : 10.60 (s, 1H), 9.45 (s, 1H), 8.23 (d, $J = 2.2$ Hz, 1H), 8.05 (dd, $J = 2.2, 8.5$ Hz, 1H), 7.92 (d, $J = 8.5$ Hz, 1H), 7.76 (d, $J = 7.2$ Hz, 1H), 7.75–7.40 (m, 5H), 7.07 (d, $J = 8.5$ Hz, 1H), 5.70 (s, 1H), 3.84 (s, 3H). LRMS (ESI) m/z 363 $[M - H]^-$.

3-Methoxy-5-[(3-nitrobiphenyl-4-ylamino)methyl]benzene-1,2-diol (16). Purification by preparative TLC yielded 16 (93 mg, 51%): mp 135 °C dec. $^1\text{H NMR}$ (DMSO- d_6) δ : 8.63 (t, $J = 5.8$ Hz, 1H), 8.30 (d, $J = 2.2$ Hz, 1H), 7.83 (d, $J = 9.1$ Hz, 1H), 7.62 (d, $J = 7.2$ Hz, 2H), 7.42 (t, $J = 7.2$ Hz, 2H), 7.31 (d, $J = 7.2$ Hz, 1H), 7.17 (m, 2H), 7.02 (d, $J = 9.1$ Hz, 1H), 6.51 (s, 1H), 6.41 (s, 1H), 4.47 (d, $J = 5.8$ Hz, 2H), 3.71 (s, 3H). LRMS (ESI) m/z 365 $[M - H]^-$.

3-Nitrobiphenyl-4-carboxylic Acid (3,4-Dihydroxy-5-methoxyphenyl)amide (17). Purification by preparative TLC yielded 17 (42 mg, 22%): mp 182–184 °C. $^1\text{H NMR}$ (DMSO- d_6) δ : 10.36 (s, 1H), 9.00 (s, 1H), 8.32 (s, 1H), 8.13 (d, $J = 8.0$ Hz, 1H), 8.08 (s, 1H), 7.83–7.79 (m, 3H), 7.53 (t, $J = 6.9$ Hz, 2H), 7.48 (d, $J = 6.9$ Hz, 1H), 6.89 (d, $J = 2.2$ Hz, 1H), 6.83 (d, $J = 2.2$ Hz, 1H), 3.71 (s, 3H). LRMS (ESI) m/z 379 $[M - H]^-$.

2-(3,4-Dihydroxyphenyl)-5-[[2-(3,4-dimethoxyphenyl)ethyl]methylamino]-2-isopropylpentanenitrile (19). Purification by flash chromatography yielded 19 (53 mg, 25%): mp 135 °C dec. $^1\text{H NMR}$ (DMSO- d_6) δ : 9.06 (s, 1H), 6.98–6.69 (m, 3H), 6.66–6.55 (m, 2H), 5.17 (br s, 2H), 3.74 (s, 3H), 3.70 (s, 3H), 3.14–3.07 (m, 4H), 2.77–2.73 (m, 2H), 2.47 (s, 3H), 2.23–2.08 (m, 4H), 1.43–1.39 (m, 1H), 1.19–1.13 (m, 3H), 0.68 (d, $J = 6.3$ Hz, 3H). LRMS (ESI) m/z 425 $[M - H]^-$.

5-Methoxy-3,4-dioxocyclohexa-1,5-dienecarboxylic Acid (3-Nitrobiphenyl-4-yl)amide (18). Compound 15e (0.50 mmol) was dissolved in dry THF (8 mL) and added dropwise over 4 h via a dropping funnel to a stirring solution of orthochloranil (0.60 mmol) in dry diethyl ether (20 mL) at –30 °C. The reaction mixture was stirred at –30 °C for 2 h and then stored at –20 °C for 12 h. The orange precipitate was collected by filtration and washed with diethyl ether, affording the desired ortho-quinone derivate 18 (75 mg, 40%): mp 186 °C dec. $^1\text{H NMR}$ (DMSO- d_6) δ : 10.91 (s, 1H), 8.24 (d, $J = 2.2$ Hz, 1H), 8.08 (dd, $J = 2.2, 8.5$ Hz, 1H), 7.78–7.75 (m, 4H), 7.51 (d, $J = 7.4$ Hz, 2H), 7.44 (t, $J = 7.2$ Hz, 2H), 3.77 (s, 3H). LRMS (ESI) m/z 377 $[M - H]^-$.

Biology. Cell Culture. MDCK-MDR1 and MDCK-MRP1 cell lines were a gift from Prof. P. Borst, NKI-AVL Institute, Amsterdam, The Netherlands. MDCK-MDR1 and MDCK-MRP1 cells were grown in DMEM high glucose supplemented with 10% fetal bovine serum, 2 mM glutamine, 100 U/mL penicillin, 100 $\mu\text{g/mL}$ streptomycin in a humidified incubator at 37 °C with a 5% CO₂ atmosphere. Cell culture reagents were purchased from Celbio s.r.l. (Milano, Italy). CulturePlate 96-well plates were purchased from PerkinElmer Life Science. Calcein-AM was obtained from Sigma-Aldrich (Milan, Italy).

Calcein-AM Experiment. The experiments were carried out as described by Feng et al.³⁶ with minor modifications. Each cell line (50 000 cells per well) was seeded into black CulturePlate 96-well plates with 100 μL of medium and allowed to become confluent overnight. Test compounds were dissolved in 100 μL of culture medium and were added to the cell monolayers. The plates were then incubated at 37 °C for 30 min. Calcein-AM was added in 100 μL of phosphate-buffered saline (PBS) to yield a final concentration of 2.5 μM , and plate incubation was continued for 30 min. Each well was washed three times with ice-cold PBS. Saline buffer was added to each well, and the plates were read with a Victor3 fluorimeter (PerkinElmer) at excitation and emission wavelengths of 485 and 535 nm, respectively. Under these experimental conditions, calcein cell accumulation in the absence and presence of tested compounds was evaluated, and basal-level

fluorescence was estimated by untreated cell fluorescence. In treated wells, the increase in fluorescence was measured relative to the basal level. IC₅₀ values were determined by fitting the percent fluorescence increase percentage versus log(dose).⁴³

Compound Stability Assay. The ESI-MS measurements were performed using an electrospray interface ion trap mass spectrometer (1100 series LC/MSD trap system Agilent, Palo Alto, CA) operating in the following regime: electrospray voltage, 4.0 kV; capillary temperature, 350 °C; sample solution flow rate, 50 μ L/h.; dry gas, 5.00 L/min; nebulizer, 15.00 psi. All analyses were performed in the negative ion detection mode. Pure solvent spectrum was monitored between each two samples until the analyzed peak intensity decreased to the initial level observed before sample introduction. All reference samples were dissolved in methanol. A 50 μ L aliquot of a sample solution was injected into the instrument with a 500 μ L Hamilton syringe. After a stationary ion current level was attained, the final spectrum was obtained by averaging over 100 sequentially measured spectra.

■ ASSOCIATED CONTENT

● Supporting Information

General procedure for the Suzuki–Miyaura cross-coupling reaction, nitro group reduction by catalytic hydrogenation, benzoylation, acetylation, quaternization, and Mitsunobu reactions; Tables S1 and S2 listing spectroscopic data; Figures S1–10 showing NOESY results, relationships, mass spectra, and stability profiles; and ESI-MS method. This material is available free of charge via the Internet at <http://pubs.acs.org>.

■ AUTHOR INFORMATION

Corresponding Author

*For S.C.: phone, +39-080-5442090; fax, +39-080-5442231/0; e-mail, s.cellamare@farmchim.uniba.it. For N.A.C.: phone, +39-080-5442727; e-mail, colabufo@farmchim.uniba.it.

■ ACKNOWLEDGMENTS

Credits are due to Dr. Andrea Gissi and Dr. Antonellina Introcaso for experimental support. The authors gratefully acknowledge the financial support from European Commission (“CancerGrid” STREP project, FP VI, Contract LSHC-CT-2006-03755) and from University of Bari “Aldo Moro”, Italy (Progetto IDEA Giovani Ricercatori 2008).

■ ABBREVIATIONS USED

MDR, multidrug resistance; ABC, ATP-binding cassette; MRP1, multidrug resistance associated protein 1; P-gp, P-glycoprotein; calcein-AM, calcein acetoxymethyl ester

■ REFERENCES

- (1) Pharm, A.-N.; Penchala, S.; et al. Pharmacogenomic Characterization of ABC Transporters Involved in Multidrug Resistance. In *Multidrug Resistance: Biological and Pharmaceutical Advance in the Antitumour Treatment*; Colabufo, N. A., Ed.; Research Signpost: Kerala, India, 2008; pp 19–62.
- (2) Borst, P.; Evers, R.; Kool, M.; Wijnholds, J. A family of drug transporters: the multidrug resistance-associated proteins. *J. Natl. Cancer Inst.* **2000**, *92*, 1295–1302.
- (3) Colabufo, N. A.; Berardi, F.; Contino, M.; Niso, M.; Perrone, R. ABC pumps and their role in active drug transport. *Curr. Top. Med. Chem.* **2009**, *9*, 119–129.
- (4) Jedlitschky, G.; Leier, I.; Buchholz, U.; Barnouin, K.; Kurz, G.; Keppler, D. Transport of glutathione, glucuronate, and sulfate conjugates by the MRP gene-encoded conjugate export pump. *Cancer Res.* **1996**, *56*, 988–994.
- (5) Fernandes, J.; Gattass, C. R. Topological polar surface area defines substrate transport by multidrug resistance associated protein 1 (MRP1/ABCC1). *J. Med. Chem.* **2010**, *53*, 1883–1897.

- (6) Aller, S. G.; Yu, J.; Ward, A.; Weng, Y.; Chittaboina, S.; Zhuo, R.; Harrell, P. M.; Trinh, Y. T.; Zhang, Q.; Urbatsch, I. L.; Chang, G. Structure of P-glycoprotein reveals a molecular basis for poly-specific drug binding. *Science* **2009**, *323*, 1718–1722.

- (7) Rosenberg, M. F.; Mao, Q. C.; Holzenburg, A.; Ford, R. C.; Deeley, R. G.; Cole, S. P. C. The structure of the multidrug resistance protein 1 (MRP1/ABCC1): crystallization and single-particle analysis. *J. Biol. Chem.* **2001**, *276*, 16076–16082.

- (8) Li, Y. F.; Polgar, O.; Okada, M.; Esser, L.; Bates, S. E.; Xia, D. Towards understanding the mechanism of action of the multidrug resistance-linked half-ABC transporter ABCG2: a molecular modeling study. *J. Mol. Graphics Modell.* **2007**, *25*, 837–851.

- (9) He, S. M.; Li, R.; Kanwar, J. R.; Zhou, S. F. Structural and functional properties of human multidrug resistance protein 1 (MRP1/ABCC1). *Curr. Med. Chem.* **2011**, *18*, 439–481.

- (10) Eckford, P. D. W.; Sharom, F. J. ABC efflux pump-based resistance to chemotherapy drugs. *Chem. Rev.* **2009**, *109*, 2989–3011.

- (11) McDevitt, C. A.; Callaghan, R. How can we best use structural information on P-glycoprotein to design inhibitors? *Pharmacol. Ther.* **2007**, *113*, 429–441.

- (12) Colabufo, N. A.; Berardi, F.; Cantore, M.; Contino, M.; Inglese, C.; Niso, M.; Perrone, R. Perspectives of P-glycoprotein modulating agents in oncology and neurodegenerative diseases: pharmaceutical, biological, and diagnostic potentials. *J. Med. Chem.* **2010**, *53*, 1883–1897.

- (13) He, S.-M.; Li, R.; Kanwar, J. R.; Zhou, S.-F. Structural and functional properties of human multidrug resistance protein 1 (MRP1/ABCC1). *Curr. Med. Chem.* **2011**, *18*, 439–481.

- (14) Cole, S.; Bhardwaj, G.; Gerlach, J. H.; Mackie, J. E.; Grant, C. E.; Almquist, K. C.; Stewart, A. J.; Kurz, E. U.; Duncan, A. M.; Deeley, R. G. Overexpression of a transporter gene in a multidrug-resistant human lung cancer cell line. *Science* **1992**, *258*, 1650–1654.

- (15) Evers, R.; Kool, M.; Smith, A. J.; van Deemter, L.; de Haas, M.; Borst, P. Inhibitory effect of the reversal agents V-104, GF120918 and pluronic L61 on MDR1 P-gp-, MRP1- and MRP2-mediated transport. *Br. J. Cancer* **2000**, *83*, 366–374.

- (16) Kannan, P.; Telu, S.; Shukla, S.; Ambudkar, S. V.; Pike, V. W.; Hallidin, C.; Gottesman, M. M.; Innis, R. B.; Hall, M. D. The “specific” P-glycoprotein inhibitor tariquidar is also a substrate and an inhibitor for breast cancer resistance protein (BCRP/ABCG2). *ACS Chem. Neurosci.* **2011**, *2*, 82–89.

- (17) Draper, M. P.; Martell, R. L.; Levy, S. B. Indomethacin-mediated reversal of multidrug resistance and drug efflux in human and murine cell lines overexpressing MRP, but not P-glycoprotein. *Br. J. Cancer* **1997**, *75*, 810–815.

- (18) Gollapudi, S.; Kim, C. H.; Tran, B. N.; Sangha, S.; Gupta, S. Probenecid reverses multidrug resistance in multidrug resistance-associated protein-overexpressing HL60/AR and H69/AR cells but not in P-glycoprotein-overexpressing HL60/Tax and P388/ADR cells. *Cancer Chemother. Pharmacol.* **1997**, *40*, 150–158.

- (19) Jedlitschky, G.; Leier, I.; Buchholz, U.; Center, M.; Keppler, D. ATP-dependent transport of glutathione S-conjugates by the multidrug resistance-associated protein. *Cancer Res.* **1994**, *54*, 4833–4836.

- (20) Nakano, R.; Oka, M.; Nakamura, T.; Fukuda, M.; Kawabata, S.; Terashi, K.; Tsukamoto, K.; Noguchi, Y.; Soda, H.; Kohno, S. A. Leukotriene receptor antagonist, ONO-1078, modulates drug sensitivity and leukotriene C4 efflux in lung cancer cells expressing multidrug resistance protein. *Biochem. Biophys. Res. Commun.* **1998**, *251*, 307–312.

- (21) Dantzig, A. H.; Shepard, R. L.; Pratt, S. E.; Tabas, L. B.; Lander, P. A.; Ma, L.; Paul, D. C.; Williams, D. C.; Peng, S.-B.; Slapak, C. A.; Godinot, N.; Perry, W. L. III. Evaluation of the binding of the tricyclic isoxazole photoaffinity label LY475776 to multidrug resistance associated protein 1 (MRP1) orthologs and several ATP-binding cassette (ABC) drug transporters. *Biochem. Pharmacol.* **2004**, *67*, 1111–1121.

- (22) Norman, B. H.; Lander, P. A.; Gruber, J. M.; Kroin, J. S.; Cohen, J. D.; Jungheim, L. N.; Starling, J. J.; Law, K. L.; Self, T. D.; Tabas, L. B.;

Williams, D. C.; Paul, D. C.; Dantzig, A. H. Cyclohexyl-linked tricyclic isoxazoles are potent and selective modulators of the multidrug resistance protein (MRP1). *Bioorg. Med. Chem. Lett.* **2005**, *15*, 5526–5530.

(23) Leslie, E. M.; Mao, Q.; Oleschuk, C. J.; Deeley, R. G.; Cole, S. P. C. Modulation of multidrug resistance protein 1 (MRP1/ABCC1) transport and ATPase activities by interaction with dietary flavonoids. *Mol. Pharmacol.* **2001**, *59*, 1171–1180.

(24) Wong, I. L. K.; Chan, K. F.; Tsang, K. H.; Lam, C. Y.; Zhao, Y.; Chan, T. H.; Chow, L. M. C. Modulation of multidrug resistance protein 1 (MRP1/ABCC1)-mediated multidrug resistance by bivalent apigenin homodimers and their derivatives. *J. Med. Chem.* **2009**, *52*, 5311–5322.

(25) van Zanden, J. J.; Geraets, L.; Wortelboerb, H. M.; van Bladeren, P. J.; Rietjens, I. M. C. M.; Cnubben, N. H. P. Structural requirements for the flavonoid-mediated modulation of glutathione S-transferase P1-1 and GS-X pump activity in MCF7 breast cancer cells. *Biochem. Pharmacol.* **2004**, *67*, 1607–1617.

(26) Pick, A.; Klinkhammer, W.; Wiese, M. Specific inhibitors of the breast cancer resistance protein (BCRP). *ChemMedChem* **2010**, *5*, 1498–1505.

(27) Colabufo, N. A.; Berardi, F.; Perrone, M. G.; Cantore, M.; Contino, M.; Inglese, C.; Niso, M.; Perrone, R. Multi-drug-resistance-reverting agents: 2-aryloxazole and 2-arylthiazole derivatives as potent BCRP or MRP1 inhibitors. *ChemMedChem* **2009**, *4*, 188–195.

(28) van Zanden, J. J.; Wortelboer, H. M.; Bijlsma, S.; Punt, A.; Usta, M.; van Bladeren, P. J.; Rietjens, I. M. C. M.; Cnubben, N. H. P. Quantitative structure activity relationship studies on the flavonoid mediated inhibition of multidrug resistance proteins 1 and 2. *Biochem. Pharmacol.* **2005**, *69*, 699–708.

(29) Cerbai, G.; Di Paco, G. Su alcune ammidi degli acidi benzoico e cinnamico sostituiti. *Gazz. Chim. Ital.* **1962**, *92*, 420–427.

(30) Spehl, G.; Ixkes, U.; Pamukcu, R.; Piazza, G. A. Preparation of N,N'-Substituted Benzimidazol-2-ones for Treating Neoplasia. U.S. Patent Appl. US 20020716, 2002.

(31) McOmie, J. F. W.; Watts, M. L.; West, D. E. Demethylation of aryl methyl ethers by boron tribromide. *Tetrahedron* **1969**, *24*, 2289–2292.

(32) Cellamare, S.; Stefanachi, A.; Stolfa, D. A.; Basile, D.; Catto, M.; Campagna, F.; Sotelo, E.; Acquafredda, P.; Carotti, A. Design, synthesis, and biological evaluation of glycine-based molecular tongs as inhibitors of A β 1–40 aggregation in vitro. *Bioorg. Med. Chem.* **2008**, *16*, 4810–4822.

(33) Theodore, L. J.; Nelson, W. L. Synthesis of ¹³C-labeled verapamil compounds. *J. Labelled Compd. Radiopharm.* **1989**, *27*, 491–501.

(34) Toffoli, G.; Simone, F.; Corona, G.; Raschack, M.; Cappelletto, B.; Gigante, M.; Baiocchi, M. Structure–activity relationship of verapamil analogs and reversal of multidrug resistance. *Biochem. Pharmacol.* **1995**, *50*, 1245–1255.

(35) Barattin, R.; Perrotton, T.; Trompier, D.; Lorendeau, D.; Di Pietro, A.; du Moulinet d'Hardemare, A.; Baubichon-Cortay, H. Iodination of verapamil for a stronger induction of death, through GSH efflux, of cancer cells overexpressing MRP1. *Bioorg. Med. Chem.* **2010**, *18*, 6265–6274.

(36) Feng, B.; Mills, J. B.; Davidson, R. E.; Mireles, R. J.; Janiszewski, J. S.; Troutman, M. D.; de Moraes, S. M. In vitro P-glycoprotein assays to predict the in vivo interactions of P-glycoprotein with drugs in the central nervous system. *Drug Metab. Dispos.* **2008**, *36*, 268–275.

(37) Colabufo, N. A.; Berardi, F.; Cantore, M.; Perrone, M. G.; Contino, M.; Inglese, C.; Niso, M.; Perrone, R.; Azzariti, A.; Simone, G. M.; Paradiso, A. *Bioorg. Med. Chem.* **2008**, *16*, 3732–3743.

(38) Sebaugh, J. L. Guidelines for accurate EC₅₀/IC₅₀ estimation. *Pharm. Stat.* **2011**, *10*, 128–134.

(39) Long, L. H.; Clement, M. V.; Halliwell, B. Artifacts in cell culture: rapid generation of hydrogen peroxide on addition of (–)-epigallocatechin, (–)-epigallocatechin gallate, (+)-catechin, and quercetin to commonly used cell culture media. *Biochem. Biophys. Res. Commun.* **2000**, *25*, 50–53.

(40) Martelli, C.; Alderighi, D.; Colonnello, M.; Dei, S.; Frosoni, M.; Le Bozec, B.; Manetti, D.; Neri, A.; Romanelli, M. N.; Salerno, M.; Scapecchi, S.; Mini, E.; Sgaragli, G.; Deodori, E. N,N'-Bis(cyclohexanol)amine aryl esters: a new class of highly potent transporter-dependent multidrug resistance inhibitors. *J. Med. Chem.* **2009**, *52*, 807–817.

(41) Teodori, E.; Dei, S.; Martelli, C.; Scapecchi, S. Multidrug Resistance (MDR) Modulators: Verapamil Offsprings and Heterocyclic Derivatives. In *Multidrug Resistance: Biological and Pharmaceutical Advance in the Antitumour Treatment*; Colabufo, N. A., Ed.; Research Signpost: Kerala, India, 2008; pp 141–169.

(42) ACD/PhysChem Suite, version 7.0; Advanced Chemistry Development: Toronto, Ontario, Canada, 2003.

(43) GraphPad Prism Software, Windows version 1998; GraphPad Software Inc., San Diego, CA. U.S., 1998.